

# PEAR-SHAPED NUCLEI: NUCLEAR MODELS AND THE STANDARD MODEL\*

P.A. BUTLER

Oliver Lodge Laboratory, University of Liverpool, Liverpool L69 7ZE, UK

*(Received November 22, 2013)*

For certain combinations of protons and neutrons, there is a theoretical expectation that the shape of nuclei can assume octupole deformation, which would give rise to reflection asymmetry or a “pear shape” in the intrinsic frame, either dynamically (octupole vibrations) or statically (permanent octupole deformation). In this paper, I will briefly review the historic evidence for reflection asymmetry in nuclei, describe how recent experiments carried out at REX-ISOLDE are constraining nuclear theory and how they contribute to tests of extensions of the Standard Model, and look at future prospects for this field.

DOI:10.5506/APhysPolB.45.127

PACS numbers: 21.10.Re, 23.20.Lv, 25.70.Gh, 27.90.+b

## 1. Introduction

Strong octupole correlations leading to pear shapes can arise when nucleons near the Fermi surface occupy states of opposite parity with orbital and total angular momentum differing by 3. This condition is met for proton number  $Z \approx 34, 56$  and  $88$  and neutron number  $N \approx 34, 56, 88$  and  $134$ . The largest array of evidence for reflection asymmetry is seen at the values of  $Z \sim 88$  and  $N \approx 134$ , where phenomena such as interleaved positive- and negative-parity rotational bands in even-even nuclei [1], parity doublets in odd-mass nuclei [2], and enhanced electric-dipole (E1) transition moments [3] have been observed. Many theoretical approaches have been developed to describe the observed experimental features: shell-corrected liquid-drop models [4, 5], mean-field approaches using various interactions [6–10], models that assume  $\alpha$ -particle clustering in the nucleus [11, 12], algebraic models [13] and other semi-phenomenological approaches [14]. A broad overview of the experimental and theoretical evidence for octupole correlations is given in Ref. [15].

---

\* Presented at the XXXIII Mazurian Lakes Conference on Physics, Piaski, Poland, September 1–7, 2013.

## 2. Experimental evidence for reflection asymmetry

The observation [16], 60 years ago, of a low-lying  $1^-$  state in  $^{224}\text{Ra}$  populated by  $\alpha$ -decay led almost immediately to the suggestion (see Ref. [17] for reference) that “this state may have the same intrinsic structure as the ground state and represents a collective distortion in which the nucleus is pear-shaped”. The energy of this  $1^-$  state, while being the lowest observed of all nuclei, lies higher than that of the  $2^+$  member of the ground state rotational band. Experiments to extend both positive and negative parity bands to higher spins using nuclear reactions were carried out much later.

One of the most important indicators of whether a nucleus is reflection-asymmetric or not is the behaviour of the energy levels themselves. Alternating negative and positive parity states can arise in a number of ways from instability in the octupole degree of freedom. One limit is that the nucleus has permanent octupole deformation, in which case the component of angular momentum aligned to the rotation axis of a state having positive parity,  $i_x^+$ , or negative parity,  $i_x^-$ , is equal to the rotational angular momentum,  $R$ . In this case, the difference in aligned angular momentum,  $\Delta i_x = i_x^- - i_x^+$ , at the same rotational frequency  $\omega$ , is equal to zero. The other limit is that the negative parity band arises from octupole vibrations of the rotating (quadrupole) deformed system. Here, the negative parity states are formed by coupling  $R$  to the angular momentum of the octupole phonon ( $3\hbar$ ). If the phonon angular momentum is aligned with respect to the rotational angular momentum then  $\Delta i_x = 3\hbar$  for a given value of  $\omega$ . If the lowest negative parity band has  $K = 0$  (and this seems to provide the most favourable situation for alignment of the phonon), then the resulting spectrum can give rise to an alternating sequence of negative and positive parity states. Plots of  $\Delta i_x$  versus  $\hbar\omega$  for nuclei in the  $Z \approx 88$ ,  $N \approx 134$  mass region are given in figures 12 and 13 of Ref. [1]. As can be seen, there are several examples such as  $^{222,224,226,228}\text{Ra}$  and  $^{224,226,228,230}\text{Th}$  where the value of  $\Delta i_x$  tends to zero at low rotational frequencies. The Rn isotopes, with  $A = 218\text{--}222$ , on the other hand, are almost perfect octupole vibrators [18].

## 3. E1 and E3 moments

In order to determine the shape of nuclei, the rotational model can be used to connect the intrinsic deformation, which is not directly observable, to the electric charge moments that arise from the non-spherical charge distribution. For quadrupole deformed nuclei, the typical experimental observables are the electric-quadrupole (E2) transition moments that are related to the matrix elements connecting differing members of rotational bands in these nuclei, and E2 static moments that are related to diagonal matrix elements for a single state. If the nucleus does not change its shape under ro-

tation, both types of moments will vary with angular momentum but can be related to a constant intrinsic moment that characterizes the shape of the nucleus. For pear-shaped nuclei, there will be additionally electric-dipole (E1) and electric-octupole (E3) transition moments that connect rotational states having opposite parity. The E1 transitions can be enhanced because of the separation of the centre-of-mass and centre-of-charge. The absolute values of the E1 moments are, however, small ( $< 10^{-2}$  single particle units) and are dominated by single-particle and cancellation effects [3]. For radium isotopes, there has been a long standing prediction [3, 19] that the sign of the E1 moment changes as the mass is increased from 222 to 226. This arises from the shell correction to the bulk (droplet) contribution which becomes increasingly negative as  $N$  increases. The macroscopic-microscopic calculations successfully reproduce the near exact cancellation for the E1 moment which has been observed for  $^{224}\text{Ra}$  [20, 21]. It is, in principle, possible to measure the sign of the E1 moment relative to the E3 moment for a mixed nuclear transition. While  $\gamma$ -ray decay properties depend very weakly on the E3 admixture and Coulomb excitation at close nuclear distances has little dependence on the E1 admixture, excitation yields can become sensitive to the relative amount of E1 and E3 for an optimal distance of closest approach. At sufficiently low bombarding energy relative to the Coulomb barrier, typically 1–2 MeV per nucleon for  $^{40}\text{Ar} + ^{226}\text{Ra}$ , there is indeed sensitivity of the yields of low-lying negative parity states, following Coulomb excitation, to the E1/E3 phase. The published data [22] show a preference for the sign of  $(Q_1/Q_3)$  to be negative, although the data were not sufficiently precise to establish which hypothesis for the relative phase is the correct one.

The E3 transition moment is collective in behaviour ( $> 10$  single particle units) and is insensitive to single-particle effects, as it is generated by coherent contributions arising from the quadrupole-octupole shape. The E3 moment is, therefore, an observable that should provide direct evidence for enhanced octupole correlations and, for deformed nuclei, can be related to the intrinsic octupole deformation parameters [23]. That Coulomb excitation can be applied to the measurement of octupole shapes was first demonstrated in preliminary studies of  $^{148}\text{Nd}$  [24], in the  $Z \approx 56$ ,  $N \approx 88$  region. Until recently, E3 transition moments had been determined for only one nucleus in the  $Z \approx 88$ ,  $N \approx 134$  region,  $^{226}\text{Ra}$  [25], so that theoretical calculations of E3 moments in reflection-asymmetric nuclei had not been subject to detailed scrutiny.

#### 4. E3 experiments

Coulomb excitation is an important tool for exploring the collective behaviour of deformed nuclei that gives rise to strong enhancement of the probability of transitions between states. Traditionally, this technique has been

employed by exciting targets of stable nuclei with accelerated ion beams of stable nuclei at energies below the Coulomb barrier, ensuring that the interaction is purely electromagnetic in character. Whereas E2, E1 and magnetic dipole (M1) transition probabilities dominate in the electromagnetic decay of nuclear states, and hence can be determined from measurements of the lifetimes of the states, E2 and E3 transition moments dominate the Coulomb excitation process allowing these moments to be determined from measurement of the cross-sections of the states, often inferred from the  $\gamma$ -rays that de-excite these levels. In exceptional cases, the Coulomb excitation technique has been applied to radioactive targets like  $^{226}\text{Ra}$ , which is sufficiently long-lived (half-life 1600 yr) to produce a macroscopic sample. It is only comparatively recently that the technique has been extended to the use of accelerated beams of radioactive nuclei such as those from the Radioactive beam EXperimental facility at ISOLDE, CERN (REX-ISOLDE [26]). In order to study octupole correlations in heavy nuclei,  $^{220}\text{Rn}$  and  $^{224}\text{Ra}$  ions were produced by spallation in a thick uranium carbide target bombarded by protons from the CERN PS Booster. The ions were post-accelerated in REX-ISOLDE to an energy of 2.8 MeV per nucleon and bombarded secondary targets of  $^{60}\text{Ni}$ ,  $^{112,114}\text{Cd}$ , and  $^{120}\text{Sn}$ . The  $\gamma$ -rays emitted following the excitation of the target and projectile nuclei were detected in MINIBALL [27], an array of 24 high-purity germanium detectors, each with six-fold segmentation and arranged in eight triple-clusters. The scattered projectiles and target recoils, distinguished by their differing dependence of energy with angle measured in the laboratory frame-of-reference, were detected in a highly segmented silicon detector [28]. More details of the measurements and the GOSIA fitting procedure [29, 30] can be found in Ref. [31].

## 5. Discussion

The measured [31] values of the E2 and E3 matrix elements are all consistent with the geometric predictions expected from a rotating, deformed distribution of electric charge, although these data do not distinguish whether the negative-parity states arise from the projection of a quadrupole–octupole deformed shape or from an octupole oscillation of a quadrupole shape [32]. Figure 1 compares the experimental values of  $Q_\lambda$  derived from the matrix elements connecting the lowest states for nuclei near  $Z = 88$  and  $N = 134$  measured by Coulomb excitation. It is striking that while the E2 moment increases by a factor of 6 between  $^{208}\text{Pb}$  and  $^{234}\text{U}$ , the E3 moment changes by only 50% in the entire mass region. Nevertheless, the larger  $Q_3$  values for  $^{224}\text{Ra}$  and  $^{226}\text{Ra}$  indicate an enhancement in octupole collectivity that is consistent with an onset of octupole deformation in this mass region. On the other hand,  $^{220}\text{Rn}$  has similar octupole strength to  $^{208}\text{Pb}$ ,  $^{230,232}\text{Th}$  and  $^{234}\text{U}$ ,

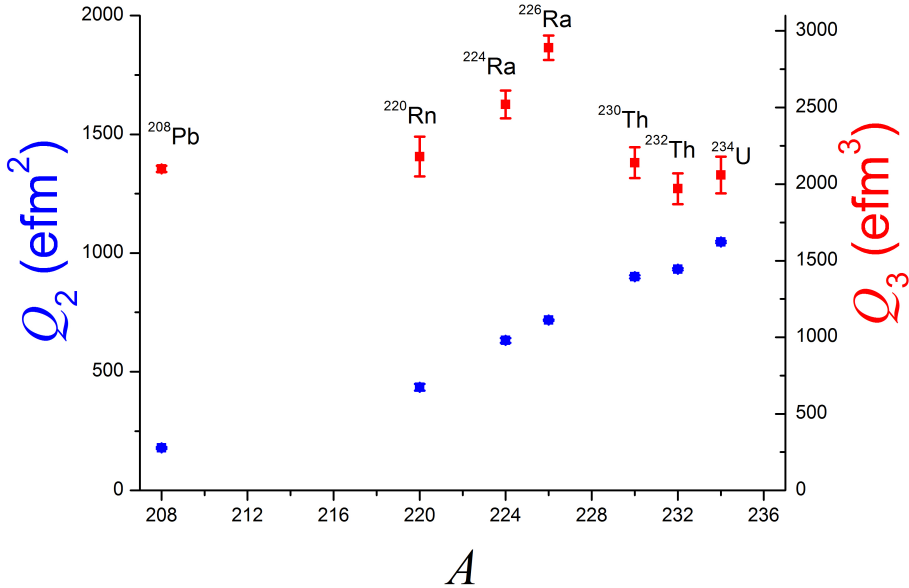


Fig. 1. The systematics of measured E2 and E3 intrinsic moments  $Q_\lambda$  for  $\lambda \rightarrow 0$  transitions. See Table 2 in Ref. [31] for details.

consistent with it being an octupole vibrator. In the case of a vibrator, the coupling of an octupole phonon to the ground state rotational band will give zero values for matrix elements such as  $\langle 1^- || E3 || 4^+ \rangle$ , because an aligned octupole phonon would couple the  $4^+$  state to a  $7^-$  state. Although the radioactive beam experiments do not have sensitivity to this quantity, this effect has been observed for  $^{148}\text{Nd}$  in the  $Z \approx 56$ ,  $N \approx 88$  octupole region [33], while for  $^{226}\text{Ra}$  the intrinsic moment derived from the measured  $\langle 1^- || E3 || 4^+ \rangle$  is similar to that derived from the value of  $\langle 0^+ || E3 || 3^- \rangle$  [25].

The values of  $Q_\lambda$ , deduced from the measured transition matrix elements, are plotted in figure 2 as a function of  $N$ . The measured  $Q_2$  values are in good agreement with several theoretical calculations, especially for  $^{224}\text{Ra}$  and the heavier radium isotopes. The trend of the experimental data for  $Q_3$  is that the values decrease from a peak near  $^{226}\text{Ra}$  with decreasing  $N$  (or  $A$ ), which is in marked contrast to the predictions of the cluster model calculations [11]. It is also at variance with the Gogny HFB mean-field predictions of a maximum for  $^{224}\text{Ra}$  [10], although the agreement with the measurements for  $^{220}\text{Rn}$  and  $^{224}\text{Ra}$  by themselves using the D1M parameterization [34] is quite good [35]. As can be seen, the relativistic mean field calculations [8] predict that the maximum value of  $Q_3$  occurs for radium isotopes between  $A = 226$  and  $230$ , depending on the parameterization, and Skyrme Hartree–Fock calculations [9] predict that  $^{226}\text{Ra}$  has the largest octupole deformation, consistent with the data.

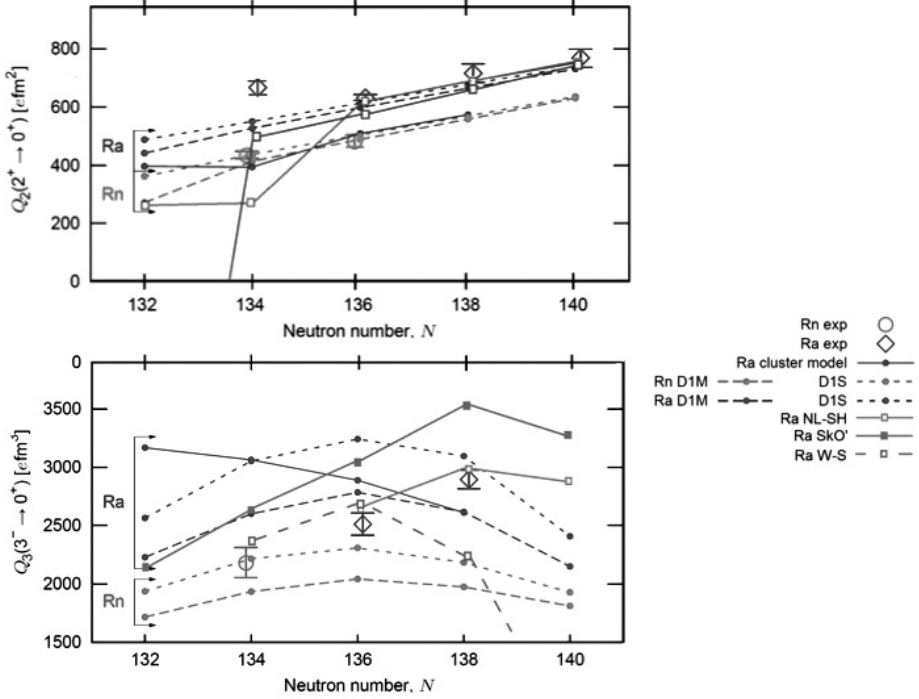


Fig. 2. Values of  $Q_2$  and  $Q_3$  for low-lying transitions as a function of  $N$ . Measured [31] values for  $\lambda \rightarrow 0$  transitions are compared to various theoretical models: cluster model [11], Gogny HFB with D1S and D1M parameterizations [10], relativistic mean field ('NL-SH') [8], Skyrme HF ('SkO') [9], and shell-corrected liquid drop models ('W-S') [4]. Note that the error bars taken from the literature for  $Q_2$  for  $^{222}\text{Rn}$  and  $^{222,228}\text{Ra}$  have been corrected from those given in Ref. [31].

Atoms with octupole-deformed nuclei are very important in the search for permanent atomic electric-dipole moments (EDMs). The observation of a non-zero EDM at the level of contemporary experimental sensitivity would indicate time-reversal (T) or, equivalently, charge-parity (CP) violation due to physics beyond the Standard Model. In fact, experimental limits on EDMs provide important constraints on many proposed extensions to the Standard Model [36, 37]. For a neutral atom in its ground state, the Schiff moment (the electric-dipole distribution weighted by radius squared [39]) is the lowest-order observable nuclear moment. Odd- $A$  octupole-deformed nuclei will have enhanced nuclear Schiff moments owing to the presence of the large octupole collectivity and the occurrence of nearly degenerate parity doublets that naturally arise if the deformation is static [38–41]. Because a CP-violating Schiff moment induces a contribution to the atomic EDM,

the sensitivity of the EDM measurement to CP violation over non-octupole-enhanced systems such as  $^{199}\text{Hg}$  [37], currently providing the most stringent limit for atoms, can be improved by a factor of 100–1000 [40]. Essential in the interpretation of such limits in terms of new physics is a detailed understanding of the structure of these nuclei. Experimental programmes are in place to measure EDMs in atoms of odd- $A$  Rn and Ra isotopes in the octupole region (see, for example, Ref. [42, 43]) but so far there is little direct information on octupole correlations in these nuclei. The recent measurements of  $Q_3$  values in  $^{220}\text{Rn}$  and  $^{224}\text{Ra}$  are consistent with suggestions from the systematic studies of energy levels [1] that the even–even isotopes  $^{218-222}\text{Rn}$  and  $^{220}\text{Ra}$  have vibrational behaviour while  $^{222-228}\text{Ra}$  have octupole-deformed character. It is concluded [31] that the parity doubling condition that leads to enhancement of the Schiff moment is unlikely to be met in  $^{219,221}\text{Rn}$ . On the other hand  $^{223,225}\text{Ra}$ , having parity doublets separated by  $\approx 50$  keV (Ref. [15]), will have large enhancement of their Schiff moments.

## 6. Summary and outlook

The recent results [31] from Coulomb excitation experiments carried out at REX-ISOLDE show that  $^{220}\text{Rn}$  has weaker octupole collectivity than  $^{224}\text{Ra}$ , and reveals detailed differences from various theoretical predictions.

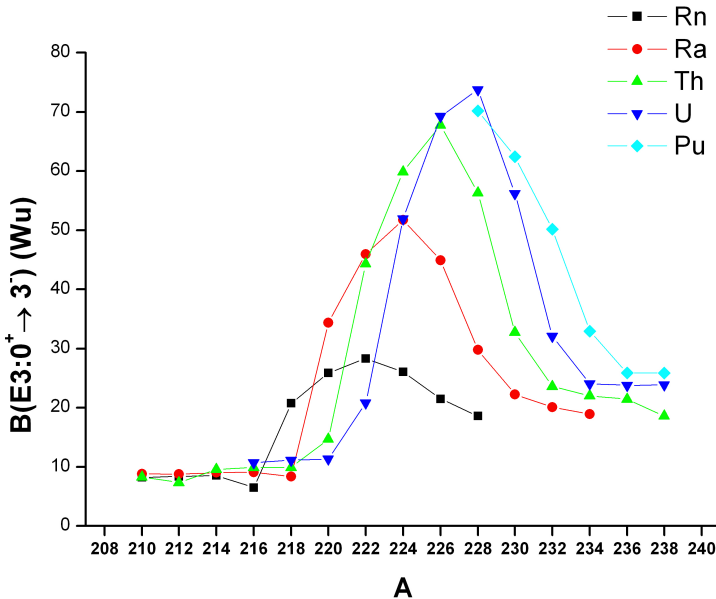


Fig. 3. Theoretical values, taken from Ref. [10], of  $B(E3 : 0^+ \rightarrow 3^-)$  transition strengths (in single particle units) *versus*  $A$  for various isotopes.

These findings should be confirmed by extending studies to other radioactive isotopes in the Rn and Ra chain, and experiments are planned to study  $^{222,228}\text{Ra}$  and  $^{222-226}\text{Rn}$  using HIE-ISOLDE. It is interesting to note that the Gogny HFB calculations [10] predict that Th and U isotopes with  $N = 134-136$ , already known to exhibit the characteristics of a rigid octupole shape [1, 44], should have significantly enhanced E3 transition strengths (70 Weisskopf units), see figure 3. The predicted yields of these isotopes from the future FRIB facility [45] will in principle be sufficient to measure the transition strengths for isotopes such as  $^{226}\text{Th}$  and  $^{228}\text{U}$ . It is also concluded [31] that  $^{219,221}\text{Rn}$  are likely to have smaller octupole-enhanced EDMs than  $^{223,225}\text{Ra}$ , though more favourable Rn candidates may emerge from future studies of the low-lying structure of heavier isotopes.

This work has been supported by the UK Science and Technology Facilities Council. I acknowledge useful discussions with the many colleagues and friends who have collaborated in the various research activities reported here, including Norah Amzal, Andrey Blazhev, Rafał Broda, Tim Chupp, Doug Cline, James Cocks, Thomas Cocolios, Tomek Czosnyka, Jacek Dobaczewski, Luis Egidio, Bogdan Fornal, Liam Gaffney, Paul Greenlees, Adam Hayes, Mark Huyse, Rich Ibbotson, Dave Jenkins, Graham Jones, Rauno Julin, Thorsten Kröll, Georg Leander, Witek Nazarewicz, Janne Pakarinen, Ray Poynter, Luis Robledo, Marcus Scheck, Frank Stephens, Thierry Stora, Nigel Warr, Fredrik Wenander, Lorenz Willmann, Hans-Jürgen Wollersheim, Ching-Yen Wu and Magda Zielińska.

## REFERENCES

- [1] J.F.C. Cocks *et al.*, *Nucl. Phys.* **A645**, 61 (1999).
- [2] M. Dahlinger *et al.*, *Nucl. Phys.* **A484**, 337 (1988).
- [3] P.A. Butler, W. Nazarewicz, *Nucl. Phys.* **A533**, 249 (1991).
- [4] W. Nazarewicz *et al.*, *Nucl. Phys.* **A429**, 269 (1984).
- [5] P. Möller *et al.*, *At. Data Nucl. Data Tables* **94**, 758 (2008).
- [6] P. Bonche, P.-H. Heenen, H. Flocard, D. Vautherin, *Phys. Lett.* **B175**, 387 (1986).
- [7] J. Egidio, L. Robledo, *Nucl. Phys.* **A494**, 85 (1989).
- [8] K. Rutz, J.A. Maruhn, P.-G. Reinhard, W. Greiner, *Nucl. Phys.* **A590**, 680 (1995).
- [9] J. Engel *et al.*, *Phys. Rev.* **C68**, 025501 (2003).
- [10] L.M. Robledo, G.F. Bertsch, *Phys. Rev.* **C84**, 054302 (2011).
- [11] T.M. Shneidman *et al.*, *Phys. Rev.* **C67**, 014313 (2003).

- [12] B. Buck, A.C. Merchant, S.M. Perez, *J. Phys. G* **35**, 085101 (2008).
- [13] N.V. Zamfir, D. Kusnezov, *Phys. Rev.* **C63**, 054306 (2001).
- [14] S. Frauendorf, *Phys. Rev.* **C77**, 021304 (2008).
- [15] P.A. Butler, W. Nazarewicz, *Rev. Mod. Phys.* **68**, 349 (1996).
- [16] F. Asaro, F. Stephens, Jr., I. Perlman, *Phys. Rev.* **92**, 1495 (1953).
- [17] F.S. Stephens, Jr., F. Asaro, I. Perlman, *Phys. Rev.* **100**, 1543 (1955).
- [18] J.F.C. Cocks *et al.*, *Phys. Rev. Lett.* **78**, 2920 (1997).
- [19] G. Leander *et al.*, *Nucl. Phys.* **A453**, 58 (1986).
- [20] R.J. Poynter *et al.*, *Phys. Lett.* **B232**, 447 (1989).
- [21] M. Marten-Tölle *et al.*, *Z. Phys.* **A336**, 27 (1990).
- [22] N. Amzal *et al.*, *Nucl. Phys.* **A734**, 465 (2004).
- [23] L.M. Robledo, G.F. Bertsch, *Phys. Rev.* **C86**, 054306 (2012).
- [24] P.A. Butler, *Heavy Ions in Nuclear and Atomic Physics*, eds. Z. Wilhelmi, G. Szeftlińska (Adam Hilger), 1989, p. 295.
- [25] H.J. Wollersheim *et al.*, *Nucl. Phys.* **A556**, 261 (1993).
- [26] D. Voulot *et al.*, *Nucl. Instrum. Methods* **B266**, 4103 (2008).
- [27] N. Warr *et al.*, *Eur. Phys. J.* **A49**, 40 (2013).
- [28] A. Ostrowski *et al.*, *Nucl. Instrum. Methods* **A480**, 448 (2002).
- [29] T. Czosnyka, D. Cline, C.Y. Wu, *Bull. Am. Phys. Soc.* **28**, 745 (1983).
- [30] D. Cline, *Nucl. Phys.* **A557**, 615 (1993).
- [31] L.P. Gaffney *et al.*, *Nature* **497**, 199 (2013).
- [32] W. Nazarewicz, S.L. Tabor, *Phys. Rev.* **C45**, 2226 (1992).
- [33] R.W. Ibbotson *et al.*, *Nucl. Phys.* **A619**, 213 (1997).
- [34] S. Goriely, S. Hilaire, M. Girod, S. Péru, *Phys. Rev. Lett.* **102**, 242501 (2009).
- [35] L.M. Robledo, P.A. Butler, *Phys. Rev.* **C88**, 051302(R) (2013).
- [36] M. Pospelov, A. Ritz, *Ann. Phys.* **318**, 119 (2005).
- [37] W.C. Griffith *et al.*, *Phys. Rev. Lett.* **102**, 101601 (2009).
- [38] W.C. Haxton, E.M. Henley, *Phys. Rev. Lett.* **51**, 1937 (1983).
- [39] V. Spevak, N. Auerbach, V.V. Flambaum, *Phys. Rev.* **C56**, 1357 (1997).
- [40] J. Dobaczewski, J. Engel, *Phys. Rev. Lett.* **94**, 232502 (2005).
- [41] J. Ellis, J. Lee, A. Pilaftsis, *J. High Energy Phys.* **0211**, 045 (2011).
- [42] J.R. Guest *et al.*, *Phys. Rev. Lett.* **98**, 093001 (2007).
- [43] H.W. Wilschut *et al.*, *Nucl. Phys.* **A844**, 143c (2010).
- [44] P.T. Greenlees *et al.*, *J. Phys. G* **24**, L63 (1998).
- [45] [http://frib.msu.edu/sites/default/files/FRIB\\_Opening\\_New\\_Frontiers\\_in\\_Nuclear\\_Science.pdf](http://frib.msu.edu/sites/default/files/FRIB_Opening_New_Frontiers_in_Nuclear_Science.pdf)